Low-Temperature Recombination of Electrons and Donors in *n*-Type Germanium and Silicon*

R. A. Brown† and Sergio Rodriguez
Department of Physics, Purdue University, Lafayette, Indiana
(Received 15 July 1966; revised manuscript received 3 August 1966)

We give a revised calculation of the recombination cross section of a conduction electron and an ionized donor impurity in *n*-type Ge and Si at liquid-helium temperatures. The energy-band structure of Ge and Si is taken into account and we show that the polarization of the phonons, which are emitted during the recombination process, is of great importance. The calculated cross sections agree reasonably well with experiment as regards temperature dependence, although the order-of-magnitude agreement is not as good.

I. INTRODUCTION

A CLASSICAL theory of electron-donor recombination in semiconductors was first discussed by Lax,[1] and later by Hamann and McWhorter[2] (HM). With regard to the quantum-mechanical formulation, a model for the electron-donor recombination process has been developed by Ascarelli and Rodriguez[3] (AR), and later modified by one of the authors.[4] In a forthcoming paper,[5] one of us has shown that the purely classical theory of HM apparently contains a number of serious defects.

The purpose of the present article is to present an improved and more comprehensive version of the work of AR. In particular, the effect of the energy-band structure of Ge and Si on the form of the electron-lattice interaction is taken into account.

Following AR, we calculate the recombination cross section of a conduction electron, having a spherical effective mass m^*, and a donor impurity whose bound states are taken to be hydrogen-like. Recombination occurs with the initial capture of a conduction electron in an excited (but not necessarily a highly excited) donor state followed by successive transitions to lower lying states, each such transition occurring with the emission of a single acoustic phonon. Only those donor wave functions corresponding to s states are used,[3,5] since electron capture in these states is more probable than in states having higher angular momentum.

It is worthwhile emphasizing that the theory of AR requires that the conduction electrons are in thermal equilibrium with the lattice. Experimentally, this implies that, initially, the donor electrons are excited into the conduction band by a weak transient external field, either an electric field or extrinsic radiation. Once the exciting field has been removed, the electrons quickly come into thermal equilibrium with the lattice by means of collisions and then recombine with the ionized donors. Also, Auger (or impact) recombination of electrons[6] has been neglected; this approximation is valid at low temperatures, using weak exciting fields, and for samples having low donor concentrations. The question as to whether the various experiments on electron recombination conform to these restrictions, so as to make a comparison with the theory meaningful, is discussed elsewhere.[5]

In Sec. II we calculate the capture cross section for a conduction electron in an excited donor state. Section III deals with the probability that once an electron is captured it will stay bound to the donor. Section IV is concerned with the total recombination cross section of electrons and donors and with a comparison between theory and experiment. Finally, a brief summary of the results is given in Sec. V. Mathematical details are relegated to the appendices.

II. CAPTURE IN EXCITED STATES

Let $\sigma_c(n)$ be the cross section for the capture of a conduction electron in a stationary state, having principal quantum number n, of a donor impurity (only s states are considered). Using the principle of detailed balance one can show that[7]

$$\sigma_c(n)=\frac{\pi^2\hbar^3\beta_n}{m^*(kT)^2}\exp\left(\frac{I_n}{kT}\right), \tag{1}$$

where I_n is the ionization energy of the nth bound donor state and β_n is the probability per unit time for the thermal ionization of an electron in the nth state. The symbol T stands for the temperature in degrees *Kelvin* and k is the Boltzmann constant.

In connection with the calculation of β_n, it is known[3,4] that the fastest mechanism for thermal ionization is that which is associated with the absorption of a phonon. AR have made the simplifying assumption that only the

* This article is based on a thesis presented by Ronald A. Brown to Purdue University in partial fulfillment of the requirements for the Ph.D. degree. This work has been supported in part by the Advanced Research Projects Agency.
† Present address: Department of Metallurgy, Massachusetts Institute of Technology, Cambridge, Massachusetts.
[1] M. Lax, Phys. Rev. **119**, 1502 (1960).
[2] D. R. Hamann and A. L. McWhorter, Phys. Rev. **134**, A250 (1964).
[3] G. Ascarelli and S. Rodriguez, Phys. Rev. **124**, 1321 (1961).
[4] R. A. Brown, Ph.D. dissertation, Purdue University, 1964 (unpublished), available from University Microfilms, Ann Arbor, Michigan.
[5] R. A. Brown, Phys. Rev. **148**, 974 (1966).
[6] G. Ascarelli and S. Rodriguez, Phys. Rev. **127**, 167 (1962).
[7] For the details of this and of other derivations, the reader is referred to Ref. 4.

longitudinal acoustic phonons effectively interact with the donor electrons in the ionization process. Upon close scrutiny, this assumption turns out to be valid for the case of Si but not for Ge, as will now be discussed. The electron-lattice interaction is described by means of deformation potential theory. Let $\mathbf{s}(\mathbf{r})$ be the displacement of an atom of the lattice which occupies an equilibrium position at $\mathbf{r}$. We may expand $\mathbf{s}(\mathbf{r})$ in terms of operators representing the creation and destruction of phonon modes as follows[8]:

$$\mathbf{s}(\mathbf{r})=\left(\frac{\hbar}{2\rho V}\right)^{1/2}\sum_{q\mu}\mathbf{e}_{q\mu}(\omega_{q\mu})^{-1/2}a_{q\mu}{}^{\dagger}\times\exp(-i\mathbf{q}\cdot\mathbf{r})+\text{H.c.} \quad (2)$$

The quantities $\mathbf{e}_{q\mu}$, $\omega_{q\mu}$, and $a_{q\mu}{}^{\dagger}(a_{q\mu})$ are, respectively, a unit polarization vector, the angular frequency, and a creation (annihilation) operator associated with a phonon having wave vector $\mathbf{q}$. There are three possible polarizations $\mu(\mu=1, 2, 3)$. The assumption is made (valid only for an isotropic elastic continuum) that for each value $\mathbf{q}$ there are two possible polarizations at right angles with $\mathbf{q}$ and a third parallel to $\mathbf{q}$. V is the volume of the crystal and ρ its density.

Let H' be the change in energy of an electron in the deformed lattice. According to Herring and Vogt[9] the interaction Hamiltonian for Ge, for the case involving both longitudinal and transverse phonons, is given by

$$H'(\text{Ge})=[(\Xi_d+\tfrac{1}{3}\Xi_u)(u_{xx}+u_{yy}+u_{zz})+\tfrac{1}{3}\Xi_u(u_{yz}+u_{zx}+u_{xy})]. \quad (3)$$

Here, $u_{xx}=\partial s_x/\partial x$, $u_{xy}=\partial s_x/\partial y+\partial s_y/\partial x$, are components of the strain tensor with analogous expressions for the remaining terms. The Cartesian coordinate system xyz is chosen so that its axes are parallel to the cubic axes. Ξ_u and Ξ_d are the deformation potential constants as defined by Herring and Vogt. Equation (3) can be rewritten as

$$H'(\text{Ge})=H_L'+H_T', \quad (4)$$

where H_L' and H_T' are, respectively, the first and the second term in (3). Since the bulk deformation potential of Ge is defined by $E_1=(\Xi_d+\frac{1}{3}\Xi_u)$, it is seen that

$$H_L'=E_1\,\text{div}\mathbf{s}(\mathbf{r}), \quad (5)$$

which is exactly the interaction Hamiltonian used by AR, who considered only the effect of longitudinal phonons on the recombination process. Thus, $H'(\text{Ge})$ is separable into two parts H_L' and H_T', which take into account the effect of the longitudinal and transverse phonons, respectively. To a first approximation, H_L' and H_T' can be considered as corresponding to independent interactions, and thus treated separately. For the case of Si, the shift of the energy of a valley along the x axis is

$$H_x'(\text{Si})=[\Xi_d(u_{xx}+u_{yy}+u_{zz})+\Xi_u u_{xx}]. \quad (6)$$

For the case of Ge, the procedure for calculating β_n, using H_L', has been established.[3] With a few simplifying assumptions, this same procedure can be used for the transverse part H_T'. Equation (6) for Si presents no additional difficulties. H_T' will contain, as a factor, the expression $(e_{q\lambda x}q_y+e_{q\lambda y}q_x+\cdots)$. To first order, H_T' can be considered as having only two components, say along the x and y axes, each component being treated separately. In this manner, H_T' can be treated analogously to the treatment of H_L', except that in the transverse case there will be an additional multiplicative factor of 2 corresponding to the two possible polarizations of the transverse phonons. In this approximation, we are neglecting to average the quantities $e_{q\lambda i}q_j(i, j=x, y, z; i\neq j)$ over the angles of $e_{q\lambda i}$ with respect to the crystalline axes x, y, z. Also, one should be careful to use the correct values of the longitudinal and transverse speeds of sound c_L and c_T, respectively, which are appropriate to the particular phonon polarization under consideration. As will be seen later, the recombination cross section varies as a high inverse power of the speed of sound; the maximum values of c_L and c_T are used, in order that the cross sections be of minimum value. This will show clearly the effect to be produced by any further improvement in the calculation. In actuality, c_L and c_T should represent suitable averages for the longitudinal and transverse waves.

Let E_{1L} and E_{1T} be the effective deformation potentials for the longitudinal and transverse cases, respectively, in analogy with the bulk deformation potential E_1 as given in Eq. (5). For Ge, $E_{1L}=(\Xi_d+\frac{1}{3}\Xi_u)$; it is known with reasonable accuracy[10] that $E_{1L}=-2$ eV and $E_{1T}=6$ eV. With regard to Si, (6) can be rewritten as

$$H_x'(\text{Si})=[(\Xi_d+\Xi_u)u_{xx}+\Xi_d u_{yy}+\Xi_d u_{zz}]. \quad (7)$$

In order to transform (7) into a form similar to that of (5), and realizing that it is the square of the matrix element of H' that enters into the calculations, we define the mean longitudinal deformation potential for Si as

$$E_{1L}=[\tfrac{1}{3}\{(\Xi_d+\Xi_u)^2+2\Xi_d{}^2\}]^{1/2}. \quad (8)$$

This assumes, of course, that $E_{1T}=0$ for Si, which turns out to be an accurate approximation. From the work of Sham,[11] and of Aubrey *et al.*,[12] it is found that $\Xi_u=8.3$ eV and $\Xi_d=2.5$ eV (experimental estimate), so that $E_{1L}\simeq 6.6$ eV for Si.

For the calculation of the maximum values of c_L and c_T for Ge and Si, one uses the standard determinantal equation for the velocity of sound as a function of the

[8] Equation (2) includes a factor of $1/\sqrt{2}$ which was erroneously omitted in Eq. (17) of AR.

[9] C. Herring and E. Vogt, Phys. Rev. **101**, 944 (1956).

[10] R. W. Keyes, IBM J. Res. and Develop. **5**, 226 (1961).

[11] L. J. Sham, Proc. Phys. Soc. (London) **81**, 934 (1963).

[12] J. E. Aubrey, W. Gubler, T. Henningsen, and S. H. Koenig, Phys. Rev. **130**, 1667 (1963).

TABLE I. Values of β_n (sec^{-1}) for Ge.

Upper value transverse, lower value longitudinal phonons.

T(°K) \ n	2	3	4	5	6	7
2.0	2.61	1.49×10^{5}	8.53×10^{5}	1.52×10^{7}	4.10×10^{7}	5.32×10^{7}
	0.37	0.03×10^{5}	1.77×10^{5}	0.07×10^{7}	0.14×10^{7}	0.24×10^{7}
2.5	9.26×10	7.96×10^{5}	2.89×10^{6}	3.04×10^{7}	6.54×10^{7}	8.50×10^{7}
	1.32×10	0.15×10^{5}	0.47×10^{6}	0.14×10^{7}	0.26×10^{7}	0.39×10^{7}
3.0	1.02×10^{3}	2.49×10^{6}	6.76×10^{6}	4.97×10^{7}	9.69×10^{7}	1.20×10^{8}
	0.15×10^{3}	0.05×10^{6}	0.94×10^{6}	0.23×10^{7}	0.39×10^{7}	0.06×10^{8}
3.5	5.74×10^{3}	5.68×10^{6}	1.27×10^{7}	7.22×10^{7}	1.27×10^{8}	1.58×10^{8}
	0.83×10^{3}	0.13×10^{6}	0.15×10^{7}	0.34×10^{7}	0.05×10^{8}	0.07×10^{8}
4.0	2.11×10^{4}	1.07×10^{7}	2.06×10^{7}	9.74×10^{7}	1.63×10^{8}	1.97×10^{8}
	0.31×10^{4}	0.03×10^{7}	0.23×10^{7}	0.46×10^{7}	0.07×10^{8}	0.09×10^{8}
4.5	5.87×10^{4}	1.76×10^{7}	3.05×10^{7}	1.25×10^{8}	2.00×10^{8}	2.38×10^{8}
	0.85×10^{4}	0.05×10^{7}	0.31×10^{7}	0.06×10^{8}	0.09×10^{8}	0.11×10^{8}
5.0	1.34×10^{5}	2.64×10^{7}	4.22×10^{7}	1.54×10^{8}	2.41×10^{8}	2.79×10^{8}
	0.20×10^{5}	0.07×10^{7}	0.41×10^{7}	0.07×10^{8}	0.10×10^{8}	0.13×10^{8}
6.0	4.65×10^{5}	4.95×10^{7}	7.00×10^{7}	2.16×10^{8}	3.14×10^{8}	3.65×10^{8}
	0.68×10^{5}	0.15×10^{7}	0.62×10^{7}	0.10×10^{8}	0.14×10^{8}	0.17×10^{8}
7.0	1.14×10^{6}	7.88×10^{7}	1.03×10^{8}	2.82×10^{8}	3.97×10^{8}	4.52×10^{8}
	0.17×10^{6}	0.25×10^{7}	0.09×10^{8}	0.13×10^{8}	0.18×10^{8}	0.21×10^{8}
8.0	2.26×10^{6}	1.13×10^{8}	1.39×10^{8}	3.51×10^{8}	4.83×10^{8}	5.41×10^{8}
	0.34×10^{6}	0.04×10^{8}	0.11×10^{8}	0.17×10^{8}	0.21×10^{8}	0.26×10^{8}
9.0	3.88×10^{6}	1.52×10^{8}	1.78×10^{8}	4.23×10^{8}	5.61×10^{8}	6.31×10^{8}
	0.58×10^{6}	0.05×10^{8}	0.14×10^{8}	0.20×10^{8}	0.25×10^{8}	0.30×10^{8}
10.0	6.01×10^{6}	1.94×10^{8}	2.20×10^{8}	4.96×10^{8}	6.60×10^{8}	7.22×10^{8}
	0.90×10^{6}	0.07×10^{8}	0.17×10^{8}	0.23×10^{8}	0.29×10^{8}	0.34×10^{8}

TABLE II. Values of $\sigma_c(n)$ (cm^2) for Ge.

Upper value transverse, lower value longitudinal phonons.

T(°K) \ n	2	3	4	5	6	7
2.0	4.60×10^{-14}	2.12×10^{-13}	4.49×10^{-14}	1.74×10^{-13}	4.69×10^{-13}	1.61×10^{-13}
	0.65×10^{-14}	0.04×10^{-13}	0.93×10^{-14}	0.08×10^{-13}	0.16×10^{-13}	0.07×10^{-13}
2.5	3.51×10^{-14}	1.61×10^{-13}	4.17×10^{-14}	1.29×10^{-13}	2.78×10^{-13}	1.25×10^{-13}
	0.50×10^{-14}	0.03×10^{-13}	0.69×10^{-14}	0.06×10^{-13}	0.11×10^{-13}	0.06×10^{-13}
3.0	2.80×10^{-14}	1.28×10^{-13}	3.85×10^{-14}	1.02×10^{-13}	1.99×10^{-13}	1.02×10^{-13}
	0.40×10^{-14}	0.03×10^{-13}	0.53×10^{-14}	0.05×10^{-13}	0.08×10^{-13}	0.05×10^{-13}
3.5	2.30×10^{-14}	1.05×10^{-13}	3.54×10^{-14}	8.43×10^{-14}	1.48×10^{-13}	8.62×10^{-14}
	0.33×10^{-14}	0.02×10^{-13}	0.43×10^{-14}	0.39×10^{-14}	0.06×10^{-13}	0.40×10^{-14}
4.0	1.93×10^{-14}	8.78×10^{-14}	3.26×10^{-14}	7.17×10^{-14}	1.20×10^{-13}	7.47×10^{-14}
	0.28×10^{-14}	0.22×10^{-14}	0.36×10^{-14}	0.34×10^{-14}	0.05×10^{-13}	0.35×10^{-14}
4.5	1.65×10^{-14}	7.52×10^{-14}	3.01×10^{-14}	6.24×10^{-14}	9.99×10^{-14}	6.59×10^{-14}
	0.24×10^{-14}	0.20×10^{-14}	0.31×10^{-14}	0.29×10^{-14}	0.43×10^{-14}	0.31×10^{-14}
5.0	1.43×10^{-14}	6.54×10^{-14}	2.79×10^{-14}	5.52×10^{-14}	8.67×10^{-14}	5.89×10^{-14}
	0.21×10^{-14}	0.18×10^{-14}	0.27×10^{-14}	0.26×10^{-14}	0.37×10^{-14}	0.28×10^{-14}
6.0	1.12×10^{-14}	5.14×10^{-14}	2.42×10^{-14}	4.49×10^{-14}	6.54×10^{-14}	4.87×10^{-14}
	0.16×10^{-14}	0.16×10^{-14}	0.22×10^{-14}	0.21×10^{-14}	0.29×10^{-14}	0.23×10^{-14}
7.0	9.00×10^{-15}	4.20×10^{-14}	2.13×10^{-14}	3.79×10^{-14}	5.33×10^{-14}	4.16×10^{-14}
	1.33×10^{-15}	0.14×10^{-14}	0.18×10^{-14}	0.18×10^{-14}	0.24×10^{-14}	0.20×10^{-14}
8.0	7.45×10^{-15}	3.53×10^{-14}	1.90×10^{-14}	3.28×10^{-14}	4.51×10^{-14}	3.36×10^{-14}
	1.11×10^{-15}	0.12×10^{-14}	0.15×10^{-14}	0.15×10^{-14}	0.20×10^{-14}	0.17×10^{-14}
9.0	6.30×10^{-15}	3.03×10^{-14}	1.71×10^{-14}	2.89×10^{-14}	3.84×10^{-14}	3.22×10^{-14}
	0.94×10^{-15}	0.11×10^{-14}	0.13×10^{-14}	0.14×10^{-14}	0.17×10^{-14}	0.15×10^{-14}
10.0	5.42×10^{-15}	2.65×10^{-14}	1.56×10^{-14}	2.59×10^{-14}	3.44×10^{-14}	2.89×10^{-14}
	0.81×10^{-15}	0.10×10^{-14}	0.12×10^{-14}	0.12×10^{-14}	0.15×10^{-14}	0.14×10^{-14}

direction of propagation of the sound wave relative to the crystalline axes.[13] Using a computer to obtain the velocity eigenvalues, the maximum speeds of sound are found to be $c_L=5.59\times10^5$ cm/sec and $c_T=3.59\times10^5$ cm/sec for Ge, while $c_L=9.20\times10^5$ cm/sec for Si. The various approximations made above are reasonable for an order-of-magnitude calculation, and will not affect the temperature dependence of the cross sections significantly in any case.

Some of the details regarding the calculation of the capture cross sections are given in Appendix A. The results have been obtained for $n\leqslant7$ using Coulomb wave functions for the states in the continuum, and are listed in Tables I through IV. For Ge, the separate contributions due to the longitudinal and transverse cases are listed. In order to obtain the total value of β_n or $\sigma_c(n)$

[13] C. Kittel, *Introduction to Solid State Physics* (John Wiley & Sons, Inc., New York, 1956), 2nd ed., p. 94.

TABLE III. Values of β_n (sec^{-1}) for Si.

T(°K) \ n	2	3	4	5	6	7
2.0	5.90×10^{-12}	7.28×10^{-2}	2.51×10^{3}	2.92×10^{5}	1.92×10^{6}	6.61×10^{6}
2.5	6.22×10^{-8}	4.65	3.17×10^{4}	1.39×10^{6}	6.54×10^{6}	1.65×10^{7}
3.0	3.08×10^{-5}	7.69×10	1.72×10^{5}	4.03×10^{6}	1.49×10^{7}	3.12×10^{7}
3.5	2.64×10^{-3}	5.89×10^{2}	5.83×10^{5}	8.75×10^{6}	2.70×10^{7}	5.02×10^{7}
4.0	7.54×10^{-2}	2.80×10^{3}	1.46×10^{6}	1.58×10^{7}	4.05×10^{7}	7.31×10^{7}
4.5	1.04	9.69×10^{3}	3.00×10^{6}	2.54×10^{7}	5.75×10^{7}	9.91×10^{7}
5.0	8.49	2.68×10^{4}	5.34×10^{6}	3.74×10^{7}	7.84×10^{7}	1.28×10^{8}
6.0	2.03×10^{2}	1.30×10^{5}	1.30×10^{7}	6.82×10^{7}	1.25×10^{8}	1.92×10^{8}
7.0	1.99×10^{3}	4.26×10^{5}	2.49×10^{7}	1.07×10^{8}	1.80×10^{8}	2.63×10^{8}
8.0	1.12×10^{4}	1.08×10^{6}	4.07×10^{7}	1.52×10^{8}	2.42×10^{8}	3.39×10^{8}
9.0	4.32×10^{4}	2.27×10^{6}	6.14×10^{7}	2.03×10^{8}	3.08×10^{8}	4.19×10^{8}
10.0	1.28×10^{5}	4.21×10^{6}	8.53×10^{7}	2.59×10^{8}	3.90×10^{8}	5.02×10^{8}

TABLE IV. Values of $\sigma_c(n)$ (cm^2) for Si.

T(°K) \ n	2	3	4	5	6	7
2.0	1.36×10^{-13}	2.01×10^{-14}	1.04×10^{-13}	2.06×10^{-13}	1.48×10^{-13}	1.34×10^{-13}
2.5	1.07×10^{-13}	1.47×10^{-14}	8.74×10^{-14}	1.48×10^{-13}	1.19×10^{-13}	1.02×10^{-13}
3.0	8.79×10^{-14}	1.15×10^{-14}	7.31×10^{-14}	1.13×10^{-13}	9.55×10^{-14}	8.22×10^{-14}
3.5	7.43×10^{-14}	9.55×10^{-15}	6.18×10^{-14}	9.05×10^{-14}	7.88×10^{-14}	6.45×10^{-14}
4.0	6.42×10^{-14}	8.26×10^{-15}	5.27×10^{-14}	7.48×10^{-14}	6.32×10^{-14}	5.86×10^{-14}
4.5	5.63×10^{-14}	7.38×10^{-15}	4.58×10^{-14}	6.34×10^{-14}	5.37×10^{-14}	5.11×10^{-14}
5.0	5.00×10^{-14}	6.76×10^{-15}	3.99×10^{-14}	5.48×10^{-14}	4.74×10^{-14}	4.53×10^{-14}
6.0	4.07×10^{-14}	5.98×10^{-15}	3.16×10^{-14}	4.28×10^{-14}	3.76×10^{-14}	3.69×10^{-14}
7.0	3.40×10^{-14}	5.51×10^{-15}	2.60×10^{-14}	3.49×10^{-14}	3.13×10^{-14}	3.12×10^{-14}
8.0	2.90×10^{-14}	5.19×10^{-15}	2.18×10^{-14}	2.94×10^{-14}	2.69×10^{-14}	2.70×10^{-14}
9.0	2.52×10^{-14}	4.95×10^{-15}	1.89×10^{-14}	2.54×10^{-14}	2.35×10^{-14}	2.38×10^{-14}
10.0	2.22×10^{-14}	4.75×10^{-15}	1.66×10^{-14}	2.23×10^{-14}	2.16×10^{-14}	2.12×10^{-14}

in this case, one needs only to add together the contributions due to the two phonon polarizations; for example, the total value of β_3 at 4.5°K is 1.81×10^{7} sec^{-1}.

III. STICKING PROBABILITY

Once a conduction electron has been captured in a bound state it may either remain attached to the impurity center or it may be reionized by the absorption of a phonon. Let P_n be the probability that an electron in the bound (s) state characterized by the principal quantum number n will not be ionized into the conduction band; P_n is called the "sticking probability" of the electron in the nth bound state. Let $P_n^{(\nu)}$ be the probability for ionization after ν transitions of the electron between the state n and other bound states $n'\neq n$. It follows that, for each n,

$$P_n+\sum_{\substack{\nu=1\\ n\leqslant 7}}^{\infty} P_n^{(\nu)}=1. \tag{9}$$

Further, let $P_{nn'}$ be the probability for the electronic transition from the bound state n to the state n', so that

$$P_n^{(\nu)}=\sum_{\substack{n'\neq n\\ n,n'\leqslant 7}} P_{nn'}P_{n'}^{(\nu-1)}. \tag{10}$$

If $W_{nn'}$ is the probability, per unit time, that an electron in the state n will make a transition to the state n', it follows that

$$P_{nn'}=W_{nn'}/\Big(\sum_{\substack{n'\neq n\\ n,n'\leqslant 7}} W_{nn'}+\beta_n\Big). \tag{11}$$

Also,

$$P_n^{(1)}=\beta_n/\Big(\sum_{\substack{n'\neq n\\ n,n'\leqslant 7}} W_{nn'}+\beta_n\Big), \tag{12}$$

where β_n is given by Eq. (A17). Accordingly, in order to calculate the sticking probabilities P_n, it is necessary to obtain the transition rates $W_{nn'}$; once these latter quantities are known, Eqs. (9) through (12) can be solved to

TABLE V. Values of P_n for Ge.

T(°K) \ n	2	3	4	5	6	7
2.0	1.000	1.000	0.998	0.993	0.970	0.928
2.5	1.000	1.000	0.994	0.982	0.948	0.905
3.0	1.000	0.999	0.987	0.964	0.930	0.887
3.5	0.999	0.998	0.975	0.927	0.875	0.828
4.0	0.998	0.995	0.960	0.884	0.810	0.742
4.5	0.995	0.990	0.941	0.856	0.772	0.697
5.0	0.990	0.984	0.919	0.814	0.715	0.630
6.0	0.973	0.966	0.868	0.741	0.629	0.540
7.0	0.950	0.943	0.814	0.627	0.473	0.358
8.0	0.922	0.918	0.761	0.498	0.323	0.201
9.0	0.894	0.893	0.711	0.371	0.210	0.107
10.0	0.866	0.864	0.666	0.287	0.127	0.037

TABLE VI. Values of P_n for Si.

T(°K) \ n	2	3	4	5	6	7
2.0	1.0000	1.0000	1.0000	1.0000	1.0000	1.0000
2.5	1.0000	1.0000	1.0000	1.0000	1.0000	1.0000
3.0	1.0000	1.0000	0.9999	0.9995	0.9991	0.9984
3.5	1.0000	1.0000	0.9996	0.9988	0.9978	0.9966
4.0	1.0000	1.0000	0.9989	0.9970	0.9935	0.9890
4.5	1.0000	1.0000	0.9977	0.9940	0.9860	0.9780
5.0	1.0000	1.0000	0.9959	0.9882	0.9750	0.9590
6.0	1.0000	0.9999	0.9901	0.9637	0.9297	0.8877
7.0	1.0000	0.9995	0.9812	0.9330	0.8725	0.8125
8.0	1.0000	0.9988	0.9695	0.9003	0.8157	0.7347
9.0	0.9999	0.9975	0.9548	0.8670	0.7620	0.6650
10.0	0.9998	0.9953	0.9382	0.8347	0.7183	0.6000

TABLE VII. Representative values of $W_{nn'}$ (sec^{-1}) for Ge.

Upper value transverse, lower value longitudinal phonons.

T(°K) \ $W_{nn'}$	W_{32}	W_{34}	W_{42}	W_{23}
2.0	2.92×10^{9}	1.03×10^{3}	5.40×10^{8}	2.34×10^{5}
	3.44×10^{7}	1.60×10^{5}	2.49×10^{7}	2.76×10^{3}
3.0	2.92×10^{9}	3.40×10^{3}	5.40×10^{8}	5.44×10^{6}
	3.44×10^{7}	5.20×10^{5}	2.49×10^{7}	6.41×10^{4}
4.0	2.94×10^{9}	6.40×10^{3}	5.41×10^{8}	2.64×10^{7}
	3.47×10^{7}	9.92×10^{5}	2.50×10^{7}	3.11×10^{5}
5.0	2.99×10^{9}	9.80×10^{3}	5.44×10^{8}	6.87×10^{7}
	3.52×10^{7}	1.52×10^{6}	2.51×10^{7}	8.09×10^{5}
6.0	3.05×10^{9}	1.34×10^{4}	5.48×10^{8}	1.32×10^{8}
	3.59×10^{7}	2.08×10^{6}	2.53×10^{7}	1.55×10^{6}
7.0	3.13×10^{9}	1.72×10^{4}	5.55×10^{8}	2.11×10^{8}
	3.69×10^{7}	2.66×10^{6}	2.56×10^{7}	2.49×10^{6}
8.0	3.22×10^{9}	2.10×10^{4}	5.64×10^{8}	3.05×10^{8}
	3.80×10^{7}	3.25×10^{6}	2.60×10^{7}	3.59×10^{6}
9.0	3.33×10^{9}	2.49×10^{4}	5.74×10^{8}	4.09×10^{8}
	3.92×10^{7}	3.86×10^{6}	2.65×10^{7}	4.82×10^{6}
10.00	3.44×10^{9}	2.88×10^{4}	5.86×10^{8}	5.21×10^{8}
	4.05×10^{7}	4.46×10^{6}	2.71×10^{7}	6.14×10^{6}

TABLE VIII. Representative values of $W_{nn'}$ (sec^{-1}) for Si.

T(°K) \ $W_{nn'}$	W_{43}	W_{34}	W_{23}	W_{32}
2.0	2.51×10^{7}	3.77×10^{3}	1.24×10^{-3}	8.10×10^{8}
3.0	2.51×10^{7}	6.66×10^{4}	4.68×10	8.10×10^{8}
4.0	2.54×10^{7}	3.11×10^{5}	3.10×10^{3}	8.10×10^{8}
5.0	2.58×10^{7}	7.64×10^{5}	3.48×10^{4}	8.11×10^{8}
6.0	2.65×10^{7}	1.41×10^{6}	1.86×10^{5}	8.11×10^{8}
7.0	2.73×10^{7}	2.21×10^{6}	6.14×10^{5}	8.11×10^{8}
8.0	2.82×10^{7}	3.13×10^{6}	1.51×10^{6}	8.12×10^{8}
9.0	2.92×10^{7}	4.13×10^{6}	3.05×10^{6}	8.14×10^{8}
10.0	3.03×10^{7}	5.21×10^{6}	5.34×10^{6}	8.16×10^{8}

yield P_n. Some of the details of the calculations of $W_{nn'}$ and P_n are given in Appendix B. Values for P_n are listed in Tables V and VI, while representative values of $W_{nn'}$ are listed in Tables VII and VIII. In Eqs. (9) through (12), the condition $n,n' \leqslant 7$ comes from the interimpurity cutoff, as will be discussed in the next paragraph.

With regard to overlap, it is evident that not all of the excited donor states need be considered in the electron recombination process. This is because an excited donor state having a sufficiently high principal quantum number n can have a radius which overlaps the nucleus of the closest neighboring ionized donor, so that the concept of a localized bound state breaks down. Assuming a random distribution of the ionized donors,[5] the maximum value of the principal quantum number n_0 is found to be $n_0(\text{Ge}) \approx 10$ and $n_0(\text{Si}) \approx 7$, for Ge and Si samples having acceptor concentrations of 10^{12} cm^{-3} and 10^{14} cm^{-3}, respectively. These acceptor concentrations are representative of those of samples used in electron-donor recombination experiments, as will be discussed later. In the present paper, $n_0=7$ is assumed, for simplicity.

IV. RECOMBINATION CROSS SECTION AND COMPARISON WITH EXPERIMENT

The electron recombination cross section σ_r is given by

$$\sigma_r = \sum_{n=2}^{7} P_n \sigma_c(n) . \tag{13}$$

The quantity $P_n\sigma_c(n)$ represents that portion of the capture cross section $\sigma_c(n)$ which corresponds to the electron not being ionized from the bound state n. In Eq. (13), capture into the ground state ($n=1$) is ignored, since it results in a negligible contribution to σ_r. For example, in Ge, an approximate calculation including the effects of both transverse and longitudinal phonons yields $\sigma_c(1) \cong [0.6\times10^{-14}/T(\text{°K})]\text{cm}^2$, which can be safely neglected ($P_1=1$ to a high degree of accuracy). For temperatures sufficiently above 10°K, capture in the ground state would become important compared to capture in the excited states, since the sticking probabilities P_n decrease rapidly with increasing n and with increasing T (see Tables V and VI).

In the calculation of P_n for As and Sb donors in Ge and Si, the energy of the ground state ($n=1$) of the donor can be taken from experimental values or by using the simple theoretical (Coulomb) binding energy. In Ge, for example, $E_i(\text{As})=1.27\times10^{-2}$ eV, $E_i(\text{Sb})=9.6\times10^{-3}$ eV, and $E_i(\text{Coulomb})=1.17\times10^{-2}$ eV. The only place where E_i enters into the determination of P_n is in the calculation of W_{n1}. In general, W_{n1} is small compared to $W_{nn'}$ or β_n; again in Ge, at 5°K, $W_{41}(\text{transv.}+\text{long.}) = 3.6\times10^{6}$ sec^{-1}, while $W_{42}(\text{transv.}+\text{long.})=5.7\times10^{8}$ sec^{-1} and $\beta_4(\text{total})=4.6\times10^{7}$ sec^{-1}. From the manner in which P_n was calculated in Sec. III, it is easily seen that small differences in W_{n1}, due to the particular ground-state energy used, will have little effect on the calculated values of P_n, since W_{n1} will be relatively small regardless of the value of E_i used. This assumption was verified by explicit calculation, which showed clearly that σ_r has no significant dependence on the donor binding energy. For temperatures sufficiently greater than 10°K, one should use the correct experimental donor binding energy since capture in the ground state becomes progressively more important, and capture in excited states progressively less important, as the temperature is raised.

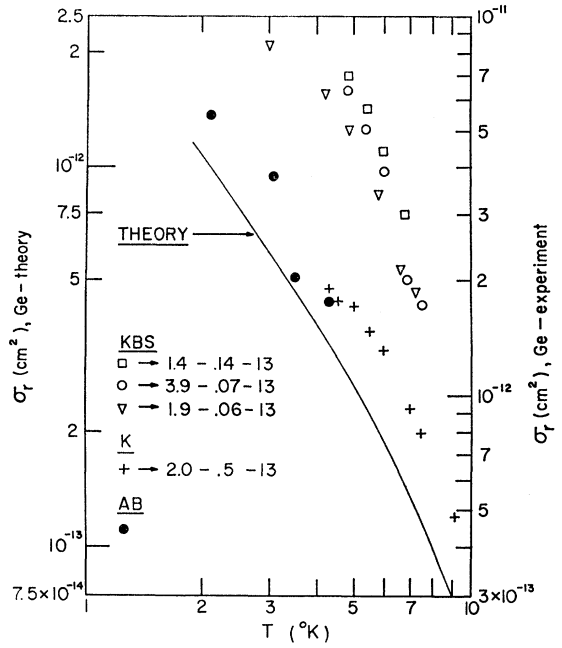

FIG. 1. Experimental and calculated values of the cross section for recombination, in Ge. Notice that the scales on the right and left of the graph are different (KBS = Koenig-Brown-Schillinger).

There have been a number of experiments on electron-donor recombination in n-type Ge[14–17] and Si.[18,19] However, many of these are such that a detailed comparison between theory and experiment is somewhat difficult. The cases of Ge and Si will be discussed separately.

A. Germanium

In Fig. 1 the theoretical curve of σ_r is compared with the experimental values as determined by Koenig[14] (K), Ascarelli and Brown[15] (AB), and Koenig, Brown, and Schillinger[17] (KBS). The theoretical curve (solid line) is taken from Table IX and does not include any effects due to impurity conduction.[5] The sample designation in Fig. 1 (and other figures) is as follows: sample 1.4–.14–13, for example, has a donor concentration $N_D=1.4\times10^{13}$ cm^{-3}, and an acceptor concentration $N_A=1.4\times10^{12}$ cm^{-3}. From Fig. 1, it is seen that the experimental and theoretical curves agree reasonably well in the temperature dependence of σ_r, although there is a disagreement in the absolute magnitude. This disagreement is not thought to be serious, since the calculated capture cross sections were deliberately minimized by choosing maximum values of the appropriate (transverse or longitudinal) speeds of sound, in order to show clearly the effect to be produced by any further improvements. In Figs. 2 and 3, $\sigma_c(n)P_n$ is plotted as a function of n, at 5 and 10°K, respectively. It is seen that for the states having $7<n\leqslant10$, there is expected to be a certain contribution to σ_r which, however, is small at the higher temperatures (a simple cutoff procedure becomes valid in the limit of high temperature). Finally, the experimental results are subject to some uncertainty, as in the work of Levitt and Honig[18] (LH) on Si. In the work of LH, the expression for determining σ_c contains the conductivity mobility μ. LH measured the Hall mobility μ_H and set $\mu_H=\mu$ although, as LH remarked, the ratio $r=\mu_H/\mu$ is known to be in the range $1<r<2$. By setting $r=1$, the results for σ_c by LH could be too large by a factor of 2. A discussion of the various experiments (on Ge) is given by KBS.

TABLE IX. Values of σ_r (cm^2) for Ge.

T(°K)	σ_r
2.0	1.13×10^{-12}
2.5	7.76×10^{-13}
3.0	5.88×10^{-13}
3.5	4.63×10^{-13}
4.0	3.72×10^{-13}
4.5	3.11×10^{-13}
5.0	2.61×10^{-13}
6.0	1.92×10^{-13}
7.0	1.36×10^{-13}
8.0	9.69×10^{-14}
9.0	7.49×10^{-14}
10.0	5.39×10^{-14}

Regarding the effect of impurity conduction, none of the experimental curves in Fig. 1 show a $T^{-1/2}$ dependence of σ_r, mainly because the temperatures were not sufficiently low.[5] The calculated curve for σ_r does not contain the effect of impurity conduction. Michel and Rosenblum[16] have obtained a temperature-independent

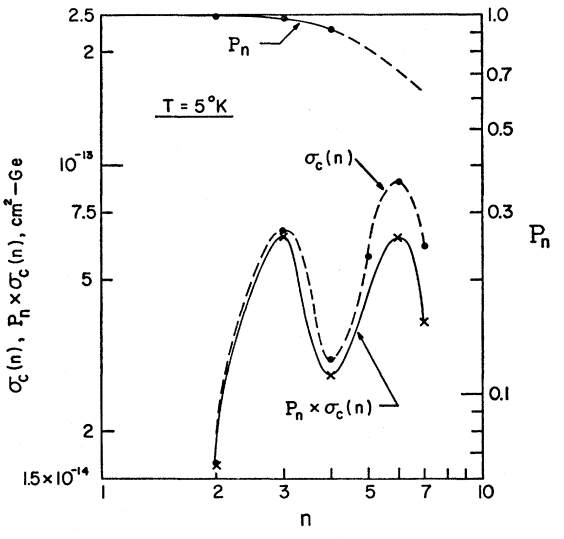

FIG. 2. $P_n\sigma_c(n)$ at 5°K for Ge.

[14] S. H. Koenig, Phys. Rev. **110**, 988 (1958).
[15] G. Ascarelli and S. C. Brown, Phys. Rev. **120**, 1615 (1960).
[16] R. E. Michel and B. Rosenblum, Bull. Am. Phys. Soc. **6**, 115 (1961).
[17] S. H. Koenig, R. D. Brown, and W. Schillinger, Phys. Rev. **128**, 1668 (1962).
[18] R. S. Levitt and A. Honig, J. Phys. Chem. Solids **22**, 269 (1961).
[19] M. Loewenstein and A. Honig, Phys. Rev. **144**, 781 (1966).

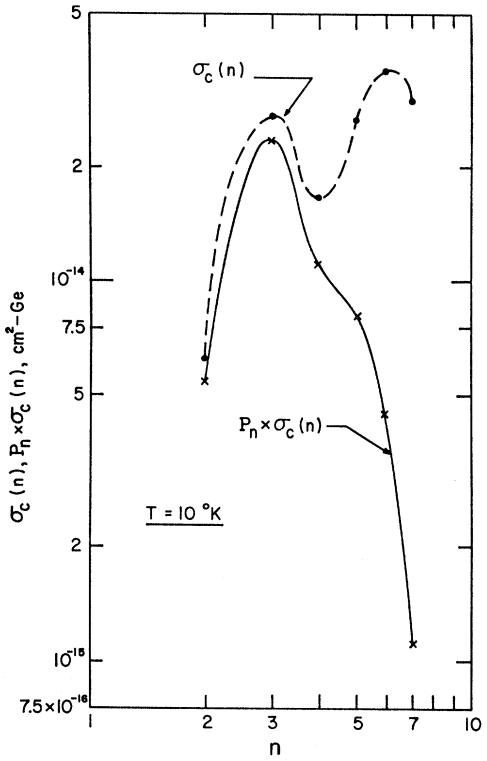

FIG. 3. $P_n\sigma_c(n)$ at 10°K for Ge.

recombination lifetime[20] in a highly purified Ge sample; unfortunately, however, a detailed account of their investigation is not yet available.

B. Silicon

Experiments on electron recombination in n-type Si (P-doped) were first carried out by Levitt and Honig[18] (LH). More recently, Loewenstein and Honig[19] obtained the capture rates of photoexcited electrons by ionized phosphorous, arsenic, antimony, and bismuth donors, as well as by neutral boron, aluminum, gallium, and indium acceptors in Si, at liquid-helium temperatures; since this work is quite detailed and comprehensive, it is best to discuss it separately, in a future paper. Only a few remarks will be made here.

The experimental values of σ_r due to LH are shown in Fig. 4, along with the theoretical curve; the calculated values for σ_r do not take impurity conduction into account. The effect of impurity conduction on the recombination cross section is apparently significant to account for the temperature dependence of σ_r, and will be discussed in a future publication. With regard to an order-of-magnitude comparison of theory with experiment, it must be remembered that the values of σ_r as determined by LH are probably too high, by as large a factor as 2 (see the section on Ge). Also, the calculated values of σ_r have been minimized. Since the theoretical and experimental approximations are such as to bring a closer agreement in the magnitude of σ_r, it is felt that the disagreement in magnitude as shown in Fig. 4 is not serious.

TABLE X. Values of σ_r (cm^2) for Si.

T(°K)	σ_r
2.0	7.48×10^{-13}
2.5	5.78×10^{-13}
3.0	4.63×10^{-13}
3.5	3.83×10^{-13}
4.0	3.20×10^{-13}
4.5	2.75×10^{-13}
5.0	2.40×10^{-13}
6.0	1.87×10^{-13}
7.0	1.50×10^{-13}
8.0	1.24×10^{-13}
9.0	1.04×10^{-13}
10.0	8.93×10^{-14}

With regard to the temperature dependence of σ_r, the results of LH show that $\sigma_r \propto T^{-1/2}$ (with the exception of sample 4.5–0.15–16), while the calculated curve yields $\sigma_r \propto T^{-1}$. This difference probably arises because the calculated curve does not include the effect of impurity conduction on σ_r. The reason why the calculated curve (see Table X) yields $\sigma_r \propto T^{-1}$ is that for sufficiently low temperatures, the excited donor states effectively act as ground states ($P_n \cong 1$, see Table VI), and

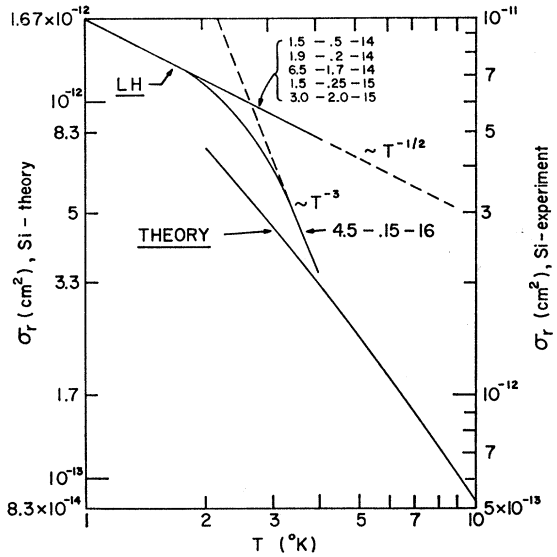

FIG. 4. Experimental and calculated values of the cross section for recombination, in Si. The effect of impurity conduction is not included (LH=Levitt-Honig).

[20] If Auger (impact) processes are neglected, the electron recombination lifetime is given by $\tau_L=(\alpha N_A)^{-1}$, where α is the capture probability and N_A=acceptor concentration. For T sufficiently less than a critical temperature (Ref. 5) T_c, τ_L, and therefore α, becomes temperature-independent. Since $\sigma_c=\alpha/\langle v\rangle$ where $\langle v\rangle \propto T^{1/2}$ is the average thermal electron velocity, $\sigma \propto T^{-1/2}$ in the extreme low-temperature limit.

it is known[21] that for the capture of a conduction electron into the ground state of a donor impurity, $\sigma_c \propto T^{-1}$.

V. CONCLUSIONS

The theory given above appears to verify, in general outline, the "giant trap" model of electron-donor recombination due originally to Lax,[1] although Lax's purely classical treatment is not thought to be sufficient for a completely accurate understanding of the recombination process. In the present work, a consideration of the energy-band structure of Ge and Si leads to the conclusion that the polarization of the phonons, emitted during the recombination process, is significant. In general, the calculated and experimentally measured recombination cross section agree reasonably well with regard to temperature dependence, although not as well as regards order of magnitude, at least for the case of germanium. For silicon we have seen that the calculated temperature dependence of the recombination cross section is in disagreement with experiments below 4.2°K. One of the authors[5] has given a discussion on the causes of this disagreement. It is suggested in Ref. 5 that this is due to the effect of impurity conduction.

Recently, Beleznay and Pataki[22] (BP) have given detailed criticisms of both the theories of Hamann and McWhorter,[2] and of Ascarelli and Rodriguez.[3,6] However, several aspects of the work of BP have been previously recognized,[4,23] and BP have neglected to discuss certain aspects of the recombination process, namely the effects of impurity conduction and of energy band structure. The work of BP is discussed in more detail in Appendix D, below.

ACKNOWLEDGMENTS

The authors would like to thank Kenneth M. Brown and Anshel Schiff for performing various computations.

APPENDIX A

Here, we calculate β_n for Ge using the transverse-phonon interaction Hamiltonian H_T'(Ge). The longitudinal cases for Ge and Si follow analogously. From Eq. (2), and using the expression for the transition probability between two quantum states within the Born approximation, it follows that

$$\beta_n=\frac{E_{1T}^2 m^*}{2(2\pi)^5\rho c_T^5\hbar^6}\int_{I_n}^{\infty} d(\hbar\omega)(\hbar\omega)^3\bar{n}(\hbar\omega)\kappa \times\int d\Omega(\mathbf{q}/|\mathbf{q}|)\int d\Omega(\boldsymbol{\kappa}/|\boldsymbol{\kappa}|)|M(\boldsymbol{\kappa},n)|^2, \quad \text{(A1)}$$

where

$$\kappa=|\boldsymbol{\kappa}|=[(2m^*/\hbar^2)(\hbar\omega-I_n)]^{1/2} \quad \text{(A2)}$$

is the wave vector of the electron in the continuum state.

The lower limit of integration for β_n in Eq. (A1) should, more properly, be $\hbar\omega=(I_n-I_7)$, because of the cutoff $n_0=7$ (see Sec. III). The absorption of phonons having energy $(I_n-I_7)\leqslant\hbar\omega\leqslant I_n$ will allow for transitions between the bound state n and the states between I_7 and zero (bottom of the conduction band), these latter states being considered as continuum states because of the nature of the interimpurity cutoff in the higher excited states. However, an approximate calculation shows that, by using the lower limit $\hbar\omega=I_n$ (rather than I_n-I_7) in Eq. (A1), an error of roughly 20% is incurred; this error is not significantly large compared with the errors incurred by other theoretical approximations and appears to be within the experimental error, and is thus felt to be consistent with the order-of-magnitude calculation presented in the present paper. The error is such that the values of β_n as determined by Eq. (A1) (see Table III, for Ge) are somewhat low.

In Eq. (A1), $\bar{n}(\hbar\omega)=[\exp(\hbar\omega/kT)-1]^{-1}$ is the number of phonons in a mode of energy $\hbar\omega$ at temperature T. The differentials $d\Omega(\mathbf{q}/|\mathbf{q}|)$, $d\Omega(\boldsymbol{\kappa}/|\boldsymbol{\kappa}|)$ are elements of solid angle along the directions of the unit vectors $\mathbf{q}/|\mathbf{q}|$ and $\boldsymbol{\kappa}/|\boldsymbol{\kappa}|$, respectively. The matrix element $M(\boldsymbol{\kappa},n)$ is given by

$$M(\boldsymbol{\kappa},n)=V^{1/2}\int d\mathbf{r}\Phi_\kappa^*\exp(i\mathbf{q}\cdot\mathbf{r})\Phi_n. \quad \text{(A3)}$$

The wave function Φ_κ is the Coulomb wave function corresponding to the wave vector $\boldsymbol{\kappa}$:

$$\Phi_\kappa=V^{-1/2}(2\pi\gamma)^{1/2}[1-\exp(-2\pi\gamma)]^{-1/2}\times\exp(i\boldsymbol{\kappa}\cdot\mathbf{r})F[i\gamma,1,i(\kappa r-\boldsymbol{\kappa}\cdot\mathbf{r})], \quad \text{(A4)}$$

where

$$\gamma=1/\kappa a^*, \quad \text{(A5)}$$

and $a^*=K\hbar^2/m^*e^2$, is the effective Bohr radius of the donor, K being the static dielectric constant of the host crystal. $\Phi_n(r)$ is the hydrogen-like wave function describing the nth bound donor (s) state:

$$\Phi_n(r)=(\pi n^3 a^{*3})^{-1/2}\exp(-r/na^*)\times F(-n+1,\,2,\,2r/na^*). \quad \text{(A6)}$$

The function $F(a,b,z)$ in (A4) and (A6) is the confluent hypergeometric function,[24] which can be written in the form[25]

$$F(i\gamma,1,z)=\frac{1}{2\pi i}\oint d\zeta\,\zeta^{i\gamma-1}(\zeta-1)^{-i\gamma}\exp(z\zeta), \quad \text{(A7)}$$

where the contour of integration contains the points

[21] H. Gummel and M. Lax, Ann. Phys. (N. Y.) **2**, 28 (1957).
[22] F. Beleznay and G. Pataki, Phys. Status Solidi **13**, 499 (1966).
[23] R. A. Brown, Bull. Am. Phys. Soc. **9**, 62 (1964).
[24] See, for example, L. D. Landau and E. M. Lifshitz, *Quantum Mechanics* (Addison-Wesley Publishing Company, Inc., Reading, Massachusetts, 1958), p. 496ff.
[25] Reference 24, p. 498, Eq. (d.8) [Eq. (A7) in the present work is obtained by making the substitutions $t=2\zeta$ and $\gamma=1$ in (d.8).]

$\zeta=0$ and $\zeta=1$ in the complex ζ plane. One can obtain $M(\kappa,n)$ as a linear combination of derivatives, with respect to a dimensionless parameter λ, of the expression

$$J_n(\lambda)=\int d\mathbf{r}\, r^{-1}\exp\left[i(\kappa-\mathbf{q})\cdot\mathbf{r}-\frac{\lambda r}{na^*}\right]\times F[i\gamma,1,i(\kappa r-\kappa\cdot\mathbf{r})], \quad \text{(A8)}$$

evaluated at $\lambda=1$. It is not difficult to show that

$$J_n(\lambda)=4\pi n^2a^{*2}[\lambda^2+(\mathbf{K}_n-\mathbf{Q}_n)^2]^{i\gamma-1}\times[Q_n{}^2+(\lambda-iK_n)^2]^{-i\gamma}, \quad \text{(A9)}$$

with

$$\mathbf{K}_n=na^*\kappa, \quad \text{(A10)}$$

$$\mathbf{Q}_n=na^*\mathbf{q}. \quad \text{(A11)}$$

Finally, it follows that[26]

$$M^*(\kappa,n)=-[1-\exp(-2\pi\gamma)]^{-1/2}(2\gamma/na^*)^{1/2}\times\sum_{\nu=0}^{n-1}\frac{2^\nu}{(\nu+1)!}\binom{n-1}{\nu}J_n{}^{(\nu+1)}, \quad \text{(A12)}$$

where $J_n{}^{(\nu)}$ is the νth derivative of $J_n(\lambda)$ with respect to λ evaluated at $\lambda=1$. The limit $\gamma\to\infty$ is taken, since at low temperatures the bulk of the contribution to the integral in (A1) occurs when $\hbar\omega\gtrsim I_n$, or when $\kappa\to 0$. In this limit, (A9) becomes

$$J_n(\lambda)=4\pi n^2a^{*2}/(\lambda^2+Q_n{}^2)\times\exp\left(-\frac{2\lambda n}{\lambda^2+Q_n{}^2}-\frac{2niQ_n\cos\theta}{\lambda^2+Q_n{}^2}\right), \quad \text{(A13)}$$

where θ is the angle between κ and $\mathbf{q}$. Finally, setting

$$M^*(\kappa,n)=M_n{}^*(2\pi/\kappa a^*)^{1/2}(\pi na^*)^{-1/2}J_n, \quad \text{(A14)}$$

$$g=2\hbar c_T/a^*kT, \quad \text{(A15)}$$

and

$$h=E_i/kT, \quad \text{(A16)}$$

it is found that

$$\beta_n(T)=\frac{E_{1T}{}^2m^*a^{*2}n^3k^4T^4}{2\pi^3\rho\hbar^6c_T{}^5}\int_{h/n^2}^{\infty}dy\, y^3[\exp(y)-1]^{-1}\times\frac{\exp\{-4n/[1+(2ny)/g]^2\}}{[1+(2ny/g)^2]^2}\int d\Omega(\mathbf{q}/|\mathbf{q}|)\times\int d\Omega(\kappa/|\kappa|)|M_n{}^*|^2. \quad \text{(A17)}$$

Through the use of a simple iterative procedure, one can obtain the quantities $J_n{}^{(\nu)}(\lambda)$ $(\nu=0, 1, \cdots, n)$ in terms of $J_n(\lambda)$ as given by (A13): from (A13),

$$\frac{J_n{}^{(1)}(\lambda)}{J_n(\lambda)}=\left[-\frac{2(\lambda+n)}{\lambda^2+Q_n{}^2}+\frac{4n\lambda^2+4n\lambda iQ_n\cos\theta}{(\lambda^2+Q_n{}^2)^2}\right]. \quad \text{(A18)}$$

Using partial fractions, (A18) becomes

$$\frac{J_n{}^{(1)}(\lambda)}{J_n(\lambda)}=\left[-\left(\frac{1}{\lambda+iQ_n}+\frac{1}{\lambda-iQ_n}\right)+\frac{n(1-\cos\theta)}{(\lambda+iQ_n)^2}+\frac{n(1+\cos\theta)}{(\lambda-iQ_n)^2}\right]. \quad \text{(A19)}$$

Taking the νth derivative of (A19) with respect to λ yields

$$\frac{d^\nu}{d\lambda^\nu}\left[\frac{J_n{}^{(1)}(\lambda)}{J_n(\lambda)}\right]=\left[(-1)^{\nu+1}\nu!\times\left\{\frac{1}{(\lambda+iQ_n)^{\nu+1}}+\frac{1}{(\lambda-iQ_n)^{\nu+1}}\right\}+(-1)^\nu(\nu+1)!\times n\left\{\frac{1-\cos\theta}{(\lambda+iQ_n)^{\nu+2}}+\frac{1+\cos\theta}{(\lambda-iQ_n)^{\nu+2}}\right\}\right]. \quad \text{(A20)}$$

The left-hand side of (A20) is determined by using Leibniz's formula. Remembering that $J_n{}^{(\nu)}(\lambda=1)\equiv J_n{}^{(\nu)}$, Eqs. (A19) and (A20) enable one to solve successively for $J_n{}^{(\nu)}$ $(\nu=0, 1, \cdots, n)$, after which one can determine the quantity $M_n{}^*$ in (A14) and (A17).

The angular integrations in (A17) can be performed easily. It is not difficult to see that $M_n{}^*$ is of the form

$$M_n{}^*=[A+B\cos^2\theta+C\cos^4\theta+\cdots+i\times\cos\theta(A'+B'\cos^2\theta+\cdots)], \quad \text{(A21)}$$

so that $|M_n{}^*|^2$ will contain only even powers of $\cos\theta$. Letting $d\Omega(\mathbf{q}/|\mathbf{q}|)=\sin\theta_1d\theta_1d\Phi_1$ and $d\Omega(\kappa/|\kappa|)=\sin\theta_2\times d\theta_2d\Phi_2$, one can write

$$P_l(\cos\theta)=\left\{P_l(\cos\theta_1)P_l(\cos\theta_2)+2\sum_{m=1}^{l}\frac{(l-m)!}{(l+m)!}P_l{}^m(\cos\theta_1)P_l{}^m(\cos\theta_2)\times\cos[m(\Phi_1-\Phi_2)]\right\}, \quad \text{(A22)}$$

where P_l, $P_l{}^m$ are the Legendre polynomials and the associated Legendre functions, respectively. Since $|M_n{}^*|^2$ contains only even powers of $\cos\theta$, and one can write terms such as $\cos^{2p}\theta$ $(p=0, 1, \cdots)$ in terms of the Legendre polynomials, it follows easily from the orthogonality properties of P_l, $P_l{}^m$, that

$$\int\int d\Omega(\mathbf{q}/|\mathbf{q}|)d\Omega(\kappa/|\kappa|)\cos^{2p}\theta=\frac{(4\pi)^2}{2p+1}. \quad \text{(A23)}$$

[26] Equation (A12) in the present work corrects a misprint in Eq. (A13) of the work of AR.

Accordingly, (A23) can be used to eliminate the angular integrations in (A17), after which (A17) can be programmed for a computer. Also, (A17) must be multiplied by a factor of 2, to account for the two possible transverse phonon polarizations, this factor being absent for the case of longitudinal phonons.

APPENDIX B

We shall first indicate some of the steps in the calculation of $W_{nn'}$ for the case of transverse phonons in Ge, it being assumed for simplicity that $n>n'$. Since for this case a phonon is created during the electron transition $n\rightarrow n'$, the interaction Hamiltonian is

$$H'=-iE_{1T}(\hbar/2\rho V)^{1/2}q(\omega_q)^{-1/2}a_q^{\dagger}\exp(-i\mathbf{q}\cdot\mathbf{r}). \quad \text{(B1)}$$

Setting $\hbar\omega_{nn'}=(E_n-E_{n'})$, and using the Born approximation as in Appendix A, it follows that

$$W_{nn'}=\frac{E_{1T}^2\omega_{nn'}^3}{8\pi^2\hbar\rho c_T^5}[1-\exp(-\hbar\omega_{nn'}/kT)]^{-1}\times\int d\Omega(\mathbf{q}/|\mathbf{q}|)|\langle n'|\exp(-i\mathbf{q}\cdot\mathbf{r})|n\rangle|^2. \quad \text{(B2)}$$

Defining

$$\beta_{nn'}=qa^*=(a^*/\hbar c_T)(E_n-E_{n'}), \quad \text{(B3)}$$

$$\varrho=\mathbf{r}/a^*, \quad \text{(B4)}$$

and realizing that the initial and final states are s states, the matrix element in (B2) takes the form

$$\langle n'|\exp(-i\mathbf{q}\cdot\mathbf{r})|n\rangle=\frac{4I_{nn'}}{\beta_{nn'}(nn')^{3/2}}, \quad \text{(B5)}$$

where

$$I_{nn'}=\int_0^{\infty}d\rho\,\rho\,\sin(\beta_{nn'}\rho)\exp\left[-\rho\left(\frac{1}{n}+\frac{1}{n'}\right)\right]\times F(-n+1,2,2\rho/n)F(-n'+1,2,2\rho/n'). \quad \text{(B6)}$$

Thus, (B2) becomes

$$W_{nn'}=\frac{8E_{1T}^2\beta_{nn'}|I_{nn'}|^2}{\pi\hbar\rho c_T^2a^{*3}(nn')^3[1-\exp(-\hbar\omega_{nn'}/kT)]}. \quad \text{(B7)}$$

Equation (B7) must be multiplied by a factor of 2 to account for the two possible transverse phonon polarizations. Notice that this factor is absent in the case of longitudinal phonons. In (B6), the hypergeometric function F is given by

$$F(-n+1,2,2\rho/n)=\sum_{\nu=0}^{n-1}c_\nu(-n+1,2)\rho^\nu, \quad \text{(B8)}$$

where

$$c_0=1, \quad \text{(B9)}$$

$$c_\nu(-n+1,2)=\left(-\frac{2}{n}\right)^\nu\frac{(n-1)(n-2)\cdots(n-\nu)}{(\nu+1)!\nu!}, \quad 1\leqslant\nu\leqslant(n-1). \quad \text{(B10)}$$

Using (B8) through (B10), one can perform an exact integration of (B6), thus determining $W_{nn'}$. Also, from the principle of detailed balance,

$$W_{n'n}=W_{nn'}\exp(-\hbar\omega_{nn'}/kT). \quad \text{(B11)}$$

Finally, since $W_{nn'}$ and β_n can be calculated, it is possible to solve for $P_{nn'}$ and $P_n^{(1)}$ from Eqs. (11) and (12), respectively. Next, the assumption is made that $P_1\approx1$, which is reasonable at liquid-helium temperatures. For example, $kT=3.45\times10^{-4}$ eV at $T=4°$K, so that $kT\ll E_i$, where E_i is the binding energy of the donor ground state ($E_i\approx10^{-2}$ eV for Ge and is larger by about a factor of 4 for Si). Since kT represents the average thermal energy available to the electron from the lattice, it is highly unlikely that an electron in the ground state of a donor will be thermally ionized into the conduction band. Also, one can reasonably set $P_1^{(1)}=P_1^{(2)}=P_1^{(3)}=P_1^{(4)}=0$. With these approximations, Eqs. (9) and (10) reduce to a system of linear homogeneous equations in the unknowns P_n, $P_n^{(2)}$, $P_n^{(3)}$, $P_n^{(4)}$, which can be solved by the method of determinants.

APPENDIX C

In the work of AR, the capture cross sections $\sigma_c(n)$ were multiplied by a degeneracy factor of 4 to account for the degeneracy of the conduction band edge in Ge, the necessity for such a factor being given in Appendix C of the work of AR. In this section, the degeneracy factor will be calculated approximately for the case of Ge, since the computations are most straightforward in this case.

It is known[4] that the original treatment of AR is only approximately correct, although their expression for β_n is reasonably accurate, particularly for Ge. Thus, we shall use their treatment in order to get a rough idea of the degeneracy factor f_n where f_n enters the definition of σ_r in the form

$$\sigma_r=\sum_{n=2}^{7}f_n\sigma_c(n)P_n. \quad \text{(C1)}$$

Let $\mathbf{K}_\alpha$ ($\alpha=1,\cdots,4$) be the wave vector from the center of the Brillouin zone to the αth minimum of the conduction band, in Ge. In harmony with the notation given earlier, $\boldsymbol{\kappa}$ is the wave vector of the electron in the continuum state, or $|\boldsymbol{\kappa}|=(2m^*/\hbar^2)^{-1/2}(\hbar\omega-E_i/n^2)^{1/2}$ [see Eq. (A2) of Appendix A]. From the derivation of β_n given in Appendix A, it is seen that in order to calculate the degeneracy factor f_n, one must evaluate the quantity

$$M^*(\boldsymbol{\kappa},\alpha';n,\alpha)=V^{1/2}\int d\mathbf{r}\Phi_\kappa(\mathbf{r})\Phi_n^*(\mathbf{r})\times\exp[-i(\mathbf{q}+\mathbf{K}_\alpha-\mathbf{K}_{\alpha'})\cdot\mathbf{r}]. \quad \text{(C2)}$$

One can show[3,4] that (C2) is approximately given by

$$|M(\kappa,\alpha';\, n,\alpha')|^2 \cong \frac{8^3\pi^2}{n^3 a^{*6}\kappa |\mathbf{q}+\mathbf{K}_\alpha-\mathbf{K}_{\alpha'}|^8} \times \exp\left(-\frac{4}{na^{*2}|\mathbf{q}+\mathbf{K}_\alpha-\mathbf{K}_{\alpha'}|^2}\right). \quad \text{(C3)}$$

From Appendix A the degeneracy factor f_n, in the nth bound donor state corresponding to the αth minimum, is given by

$$f_n = \langle \sum_{\alpha'=1}^{4} |M(\kappa,\alpha';\, n,\alpha)|^2 \rangle / |M(\kappa,\alpha;\, n,\alpha)|^2, \quad \text{(C4)}$$

where $M(\kappa,\alpha;\, n,\alpha) \equiv M(\kappa,n)$ is given by (A3). In (C4), the angular brackets $\langle\ \rangle$ mean that one should average over the angle θ between $\mathbf{q}$ and $(\mathbf{K}_\alpha - \mathbf{K}_{\alpha'})$. Also, we know that[3,4]

$$|M(\kappa,\alpha;\, n,\alpha)|^2 = \frac{8^3\pi^2}{n^3\kappa q^8 a^{*6}} \exp\left(-\frac{4}{nq^2a^{*2}}\right). \quad \text{(C5)}$$

Using Eq. (C4), f_n is found by explicit calculation to be very nearly equal to unity for $2 \leqslant n \leqslant 7$, which implies that intervalley impurity scattering is not a significant effect. However, it must be remembered that the present treatment is only approximate; for example, the periodic part of the Bloch wave function has been neglected.

APPENDIX D

Recently, Beleznay and Pataki[22] have calculated the quantities $W_{n_1 l_1}{}^{n_2 l_2}$ (n_1, $n_2 \leqslant 7$), which are the rates for the transition of an electron between the bound states having quantum numbers $(n_1 l_1)$ and $(n_2 l_2)$; accordingly, they have included bound- to bound-state transitions involving states having angular-momentum quantum number $l > 0$, in contrast to the present work where only s states are included. Using the values for $\sigma_c(n)$, β_n, speed of sound c_s, and (longitudinal) deformation potential E_1 as given by Ascarelli and Rodriguez, BP claim that the sticking probabilities P_n are greatly reduced from the corresponding values as calculated by AR. By using the approximation of AR, that

$$\sigma_c(n,l) \approx \sigma_c(n)/Q_n{}^{2l}, \quad \text{(D1)}$$

where

$$Q_n{}^2 \geqslant 188/n^2, \quad \text{(D2)}$$

BP conclude that the cross section for capture in the bound state (nl), or $\sigma_c(n,l)$, is small compared to the cross section for capture in the state $(n0)$, or $\sigma_c(n,0) \equiv \sigma_c(n)$. In this way, BP claim that the decrease of the sticking probabilities in the excited states, due to the inclusion of states having nonzero angular momentum, results in a considerable decrease in the recombination cross section in Ge from the values as stated by AR. In fact, the values of the recombination cross section as taken from Table 6 of BP indicate that $\sigma_r \sim T^{-4}$ for $3°\text{K} \leqslant T \leqslant 10°\text{K}$ and that their result for σ_r differs from experiment in absolute value by more than one order of magnitude.

It is the contention of the present authors that the work of Beleznay and Pataki, although relevant to the original work of AR, is *not relevant* to the present work. In the first place, Eqs. (D1) and (D2) of AR are known to be approximate and are not used in the present work. Furthermore, the values of β_n [and thus of $\sigma_c(n)$] have been recalculated in the present paper, and are rather different from the corresponding values as given by AR (See Ref. 3). Then too, BP use the values $c_s = 5\times10^5$ cm/sec and $E_1 = 20$ eV given by AR; these values have been changed considerably in the present work, particularly since here (in a calculation involving the band structure of Ge) a distinction between the longitudinal and transverse cases is made. Also, as has already been mentioned (see Ref. 8), a factor of $1/\sqrt{2}$ was erroneously omitted from Eq. (17) of AR, and has been corrected in the present work; however, since the formalism of AR was used by BP, their values of β_n, $\sigma_c(n)$, and $W_{n_1 l_1}{}^{n_2 l_2}$ are all too small by the factor $\frac{1}{2}$. Normally, the sticking probabilities would not be affected by the factor of $\frac{1}{2}$, since it acts as a scaling factor and cancels out in Eqs. (9) through (12). However, when the polarization of the phonons is taken into account, one must include a multiplicative factor of 2 for the transverse case when calculating the quantities (β_n,etc.) mentioned above, this factor being absent for the longitudinal case. Thus, in the present paper, the factor of $\frac{1}{2}$ will not cancel as a scaling factor, since both the longitudinal and transverse cases are considered; since BP used only the longitudinal case in their calculation of the sticking probabilities, their results are not strictly comparable to the present results.